Paper No. 1250. (quote when citing this article)
Eleventh World Conference on Earthquake Engineering
ISBN: 0 08 042822 3

SEISMIC RESPONSE ANALYSIS OF GANTRY CRANES ON CONTAINER QUAY WALLS DUE TO THE GREAT HANSHIN EARTHQUAKE

S. TANAKA and T. INATOMI

Structure Division, Port and Harbor Research Institute, Ministry of Transport,
3-1-1, Nagase, Yokosuka, 239 JAPAN

ABSTRACT

The facilities in the Port of Kobe, especially container quay walls and gantry cranes were seriously damaged due to the Great Hanshin Earthquake. This paper describes the relationship with the earthquake and those damage. Moreover, this paper deals with the dynamic behaviors and the interaction between a ground and structures (a quay wall and a crane) by seismic response analysis.

KEYWORDS

The Great Hanshin Earthquake; Container Quay Wall; Gantry Crane; Seismic Response Analysis.

DAMAGE OF CONTAINER QUAY WALLS AND GANTRY CRANES

Damage of Container Quay Walls

Container quay walls in the Port of Kobe are mostly a gravity type with concrete caissons except the Maya Wharf. **Fig. 1** shows a cross section as an example of container quay walls in the Port Island. Seaside crane rails are set on concrete blocks on the caissons. On the other hand, landside crane rails are put on reclaimed land fill or steel pipe piles.

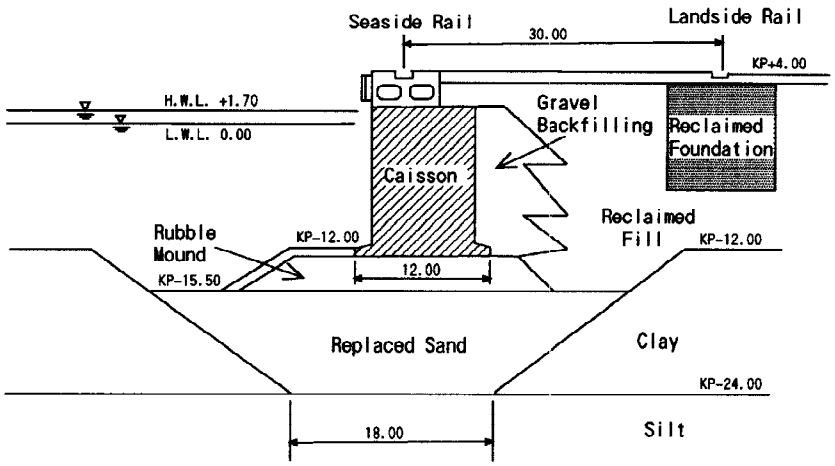

Fig. 1 Typical cross section of a container quay wall

The caissons slid seaward approximately 6 m maximum in the Rokko Island. Moreover, they inclined and subsided about 2 m maximum Similarly, ground at back sites of caissons subsided and were cracked on the surface, due to lateral deformation of the caissons. In comparison with the subsidence between two types of the landside rails, the rails on the reclaimed fill subsided similarly to the surrounding ground, however, a little subsidence of the rails on the piles left a gap between the rails and ground.

Damage of Gantry Cranes

Fig. 2 shows a arrangement of cranes at the earthquake, and **Table 1** classifies the various damages of cranes. There were 55 cranes in the Port of Kobe, which were divided into 29 middle cranes (rail span ranging from 16

to 20 m) and 26 large cranes (rail span 30 m). Categorizing them into districts, 25 cranes were in the Rokko Island, 22 cranes were in the Port Island and 8 cranes were in the Maya wharf.

Table 1 was a result of a field investigation immediately after the earthquake. In the total of 55 cranes, 22 cranes were belong to Level II which included their slightly damaged legs, and 30 cranes were belong to Level III whose legs were seriously damaged such as locally buckled plate elements. Judging from this result, it is considered that the primary damage was concentrated to legs.

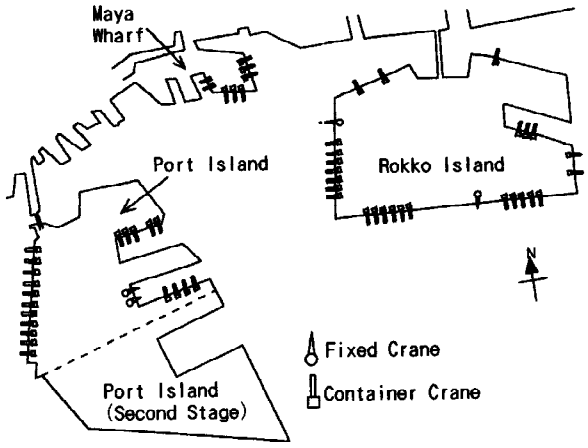

Fig. 2 Arrangement of cranes at the earthquake

Assumed Causes of Damage

Judging from damaged parts of legs, main causes of damage are assumed as follows.

Lateral Deformation of Caissons. Rail spans were expanded due to lateral deformation of caissons. Then, leg bottoms were forced to deform outside in plane perpendicular to directions of rails, as shown in x-y plane of **Fig. 3**. Therefore, local bucklings occurred around nodes connecting a leg and braces.

Rocking Vibration of Cranes. Cranes started rocking vibration due to strong motion earthquake, as shown in **Fig. 4**. Then, large section forces acted in three legs and local bucklings occurred, when one leg was lifted up. Consequently, reaction forces acted in two grounding legs toward decreasing a leg span. On the other hand, a reaction force in a leg on the up-lifted side acted toward expanding the leg span.

Table 1 Classification of damages of cranes

Leg Span	30 m		16-20 m			Total	Damaged level
Location	RI	PI	RI	PI	M		
Level I	0	0	0	0	0	0	Only derailment
Level II	4	0	1	11	6	22	Slightly damaged legs
Level III	14	7	4	4	1	30	Seriously damaged leges
Level IV	0	0	0	0	1	1	Damaged girder
Level V	1	0	0	0	0	1	Completely destroyed
Obscurity	-	-	1	-	-	1	
Total	19	7	6	15	8	55	
Location RI:Rokko Island, PI:Port Island, M:Maya Wharf							

Correlative Analyses on Assumed Causes

On assumed causes, correlative analyses are conducted for 37 cranes whose owner are Kobe Port Terminal Public Corp. **Fig. 5** show a relationship between deformation of quay walls and expansion of rail spans. Upper and lower figures indicate by rail directions and rail foundations, respectively. From these figures, the followings turn out to be clear.

1)There is a low, but a positive correlation between deformation of quay walls and expansion of rail spans.

2)Expansion of rail spans in E-W direction is greater than expansion in N-S direction.

3)Difference of rail foundations dose not affect expansion of rail spans much.

Fig. 6 indicate a relationship between expansion of both rail spans and leg spans. Upper and lower figures show by rail directions and leg spans. The followings are derived form this figure.

4)Cranes are divided into two groups; one group, whose expansion of leg spans are greater than 0 m, has a positive correlation. The another group is seemed to be not correlative and these expansion are ranging from -3.6 % (-0.57 m) to 0

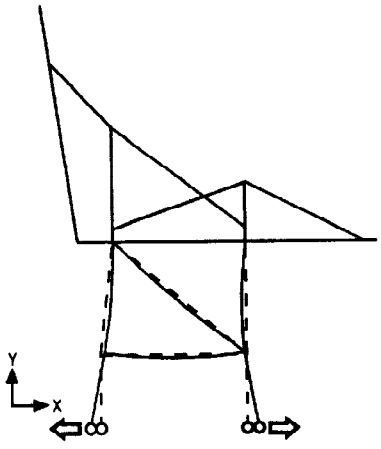

Fig. 3 Expansion of leg span

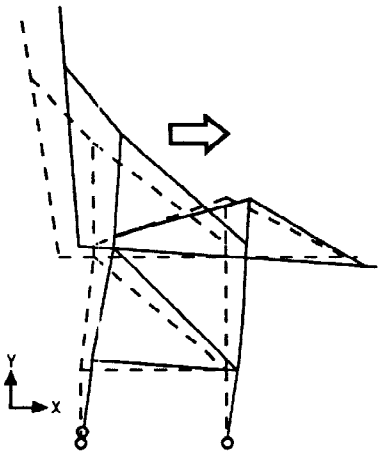

Fig. 4 Rocking of crane

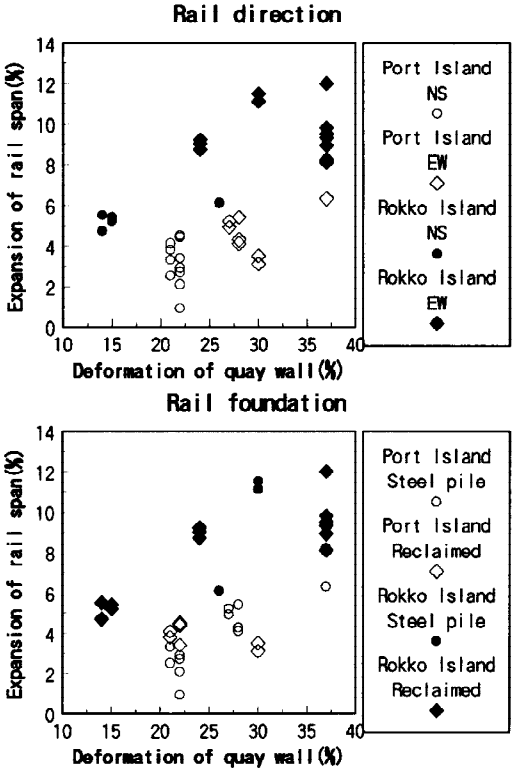

Fig. 5 Deformation of quay wall and expansion of rail span

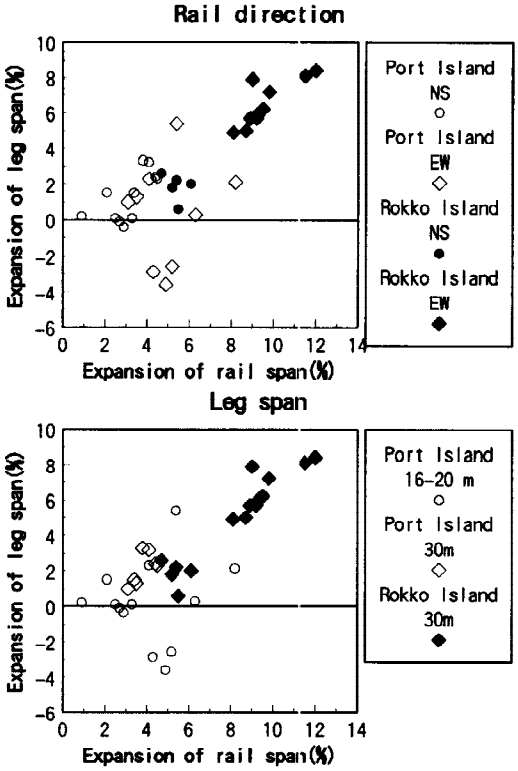

Fig. 6 Expansion of rail span and leg span

% (0 m).

5)In correlative group, most cranes have a 30 m leg span. On the contrary, leg spans of most cranes is 16 m in non-correlative group.

PROCEDURE OF SEISMIC RESPONSE ANALYSIS

Object of Seismic Response Analysis

Rocking vibration of cranes is considered to be one of main causes, as mentioned above. In order to investigate the dynamic behavior of typical cranes, seismic response analyses were conducted using with the acceleration waves of the Great Hanshin Earthquake recorded in the Port Island. One example of these analyses is described here. The nearest quay wall to the accelerograph was selected as the object of this analysis. The cross section and the location of the quay wall is shown in **Fig. 1** and **Fig. 7**.

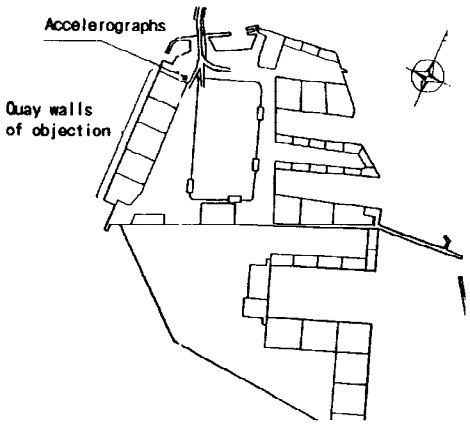

Fig. 7 Location of quay wall for objection of analysis

Model of Container Quay Wall and Base Motion

FLUSH (Lysmer *et al.* 1975), which can analyze soil-structure interaction problems, was applied to the 2-D FEM analysis. **Fig. 8** indicates vertical locations (KP +04, -12, -28 and -79 m) of four accelerographs installed on and in the ground near the quay wall, and a interactive model of both a quay wall and a crane. A model of only a quay wall (quay wall model) was also analyzed in order to compare with the interactive model. In these analyses, both left and right bounds of FEM region were defined as transmitting boundaries, in order that these bounds expressed the semi-infinite ground (so-called free fields). The bottom bound was assumed to be a rigid base.

As a base motion, the E-W component of the corrective acceleration waves was input on the bottom rigid base. These corrective components, as shown in the bottom of **Fig. 9**, was generated to rotate observed N-S and E-W components 22 degree counter-clockwise (Sugito *et al.*, to be published). The highest frequency for this analyses was 10 Hz and the iteration limit was 5 %.

Soil properties, such as an initial shear modulus G_0 and a poisson's ratio v, were determined with a result of PS logging. Shear modulus reduction factors G/G_0 and fractions of critical damping h for each effective shear strain γ_{eff} were referred to typical data for typical reclaimed lands (Coastal Development Inst. of Tech., 1993). The N-value of the reclaimed landside rail foundation was assumed to be 30.

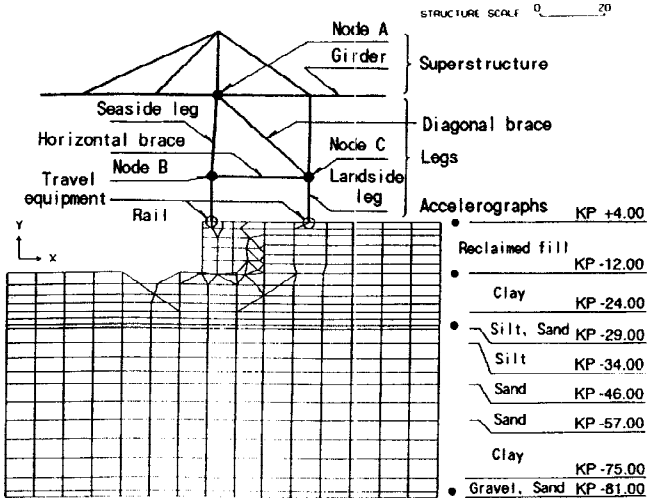

Fig. 8 Vertical location of acceleograph and interaction model of quay wall and crane

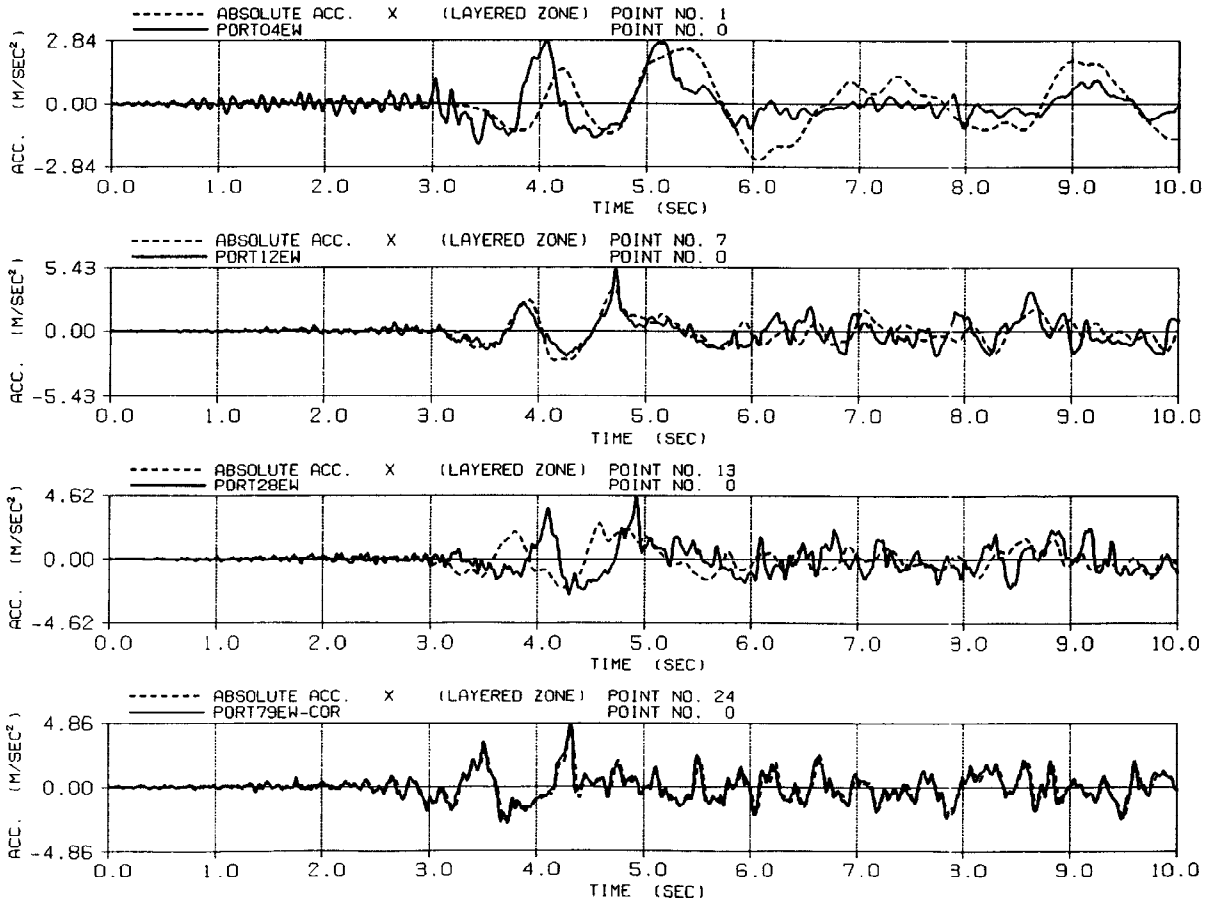

Fig. 9 Comparison with observed (solid line) and analytical waves (broken line); each depth is KP+04, -12, -28, and -79 m from top figure

Model of Gantry Crane

A typical existing crane was modeled to a 2-D elastic model in plane perpendicular to the rail direction, which were constructed with beams, masses and springs, as shown in **Fig. 8**.

In connecting conditions between the quay wall and the crane, horizontal and vertical springs were adopted and their spring factors k_h and k_v were 1.0×10^6(tf/m/m). They were estimated on the basis of the rigidity of the traveling equipments and prestressed concrete girders beneath a rail. Rotational spring factor k_θ was assumed

to be 1.0(tf·m/rad/m) so that the spring dose not confine the rotational vibration. These conditions were considered that they connected in the state of a hinge, and also that these connection could not express the actual rocking vibration such as a leg lifted up. However, a start time of the rocking vibration and the response until the time could be obtained by means of axial force time histories of leg bottoms.

RESPONSE OF CONTAINER QUAY WALL

Acceleration Response of Quay Wall

In order to examine the analytical procedure, the analytical and the observed waves of acceleration time histories on and in the ground are compared at each depth of KP +04, -12, -28 m from the top figure, as shown in **Fig. 9**. They indicates acceleration responses only for the first 10 sec in total analytical time 30 sec. In the figures, the solid lines are the observed waves and the broken lines express the analytical waves of the right free field. According to the figures, the maximum amplitudes of the analytical waves agree substantially from the observations. Furthermore, the phases of the analytical waves agree well form of the observations except the initial tremors. As the depth of the observation point shallows, the high frequency component of both analytical and observed acceleration waves decreases and the period of those waves increases. Judging from these results, it is considered that the softening of ground progresses gradually.

Deformation Response of Quay Wall

Fig. 10 indicates deformation of the quay wall at t=5.10 sec when the horizontal displacement response of seaside rail is largest. The caisson deforms most toward seaside at this time, too. The horizontal displacement are 22 cm at the seaside rail, and 27 cm at the landside rail. This figure shows that a rubble mound is compressed due to the rocking of the caisson. Moreover, the displacement of the caisson makes the land fill shear-deformed. In this analysis, the shear strain in ground is concentrated in the land fill (approximately at depth of KP -12 m) immediately on the right clay layer. The maximum effective shear strain γ_{eff} is about 1%.

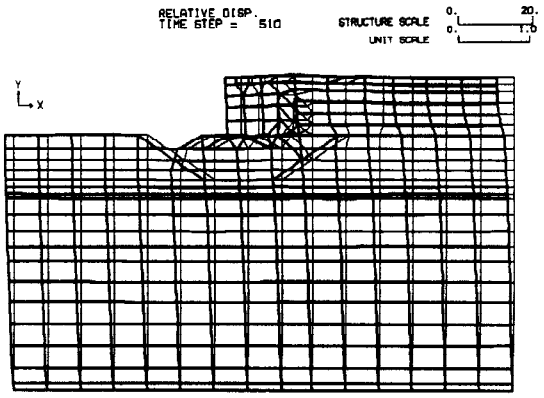

Fig. 10 Deformation of quay wall model at time of max. horizontal displacement for seaside rail (unit:m)

RESPONSE OF GANTRY CRANE

Rocking Vibration of Crane

Fig. 11 express axial force time histories of both seaside and landside leg bottoms (bottom figure) and acceleration time histories of typical points Node A and B on the legs (2 figures from top). These figures indicate only for the first 10 sec in total analytical time 30 sec. In axial force waves, compressive and tensile forces are marked with a plus and a minus sign, respectively. After time passes t=5.0 sec, axial force waves on both the seaside (solid line) and the landside (broken line) are symmetrical on the axis N=0 tf. The periods of the waves agree substantially with the natural period t=2.0 sec of the crane.

If the tensile axial force due to the vibration is equal to the compressive axial force due to the crane weight, it

is considered that the crane may start rocking. In this analysis, the compressive axial forces of legs per unit the crane width due to the dead weight are N_s=28.3 tf on the seaside and N_L=13.4 tf on the landside, respectively. It can be read from **Fig. 11** that the rocking vibration may start at t_{L1}=5.4 sec or t_{L2}=7.0 sec on the basis of the above axial force for the landside leg. Similarly, it may be at t_{S1}=6.4 sec for the seaside leg. The ratios of the maximum amplitude of tensile axial force acting immediately after t_{L1}, t_{S1} and t_{L2} to the each N_L and N_s are 1.03, 1.09 and 2.59, respectively. Judging from these ratios, the rocking is considered to start at latest until the time of the maximum amplitude soon after t_{L2}. The acceleration response of the crane is approximately ranging from -6 to 3 m/sec^2 until the rocking time.

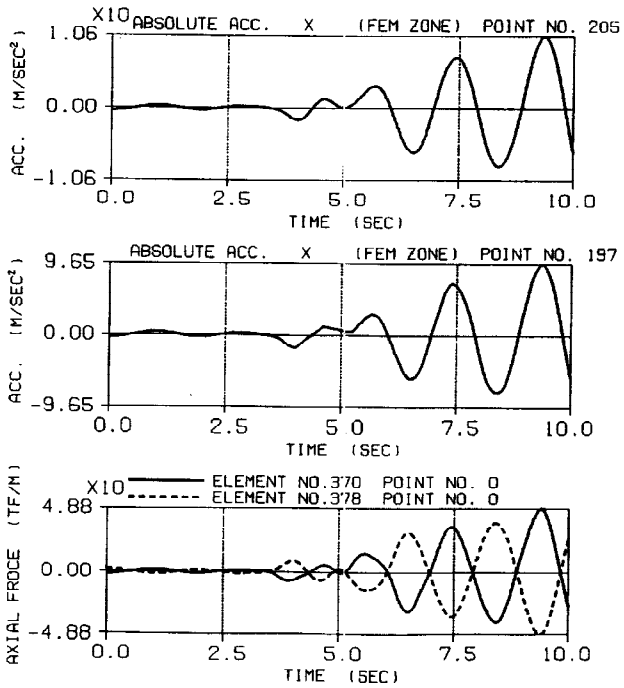

Fig. 11 Axial force waves of leg bottoms (bottom figure) and acceleration waves of Node A and B (2 figures from top)

Acceleration and Deformation Response of Crane

Fig. 12 shows acceleration vectors of the quay wall and the crane at the above t_{L1}. Approximately the same acceleration acts in legs above the horizontal brace. The diagonal brace from Node A to C increases the rigidity of legs above the horizontal brace. Moreover, the acceleration at this time acts vertically more than horizontally at both right and left ends of the girder.

Deformation of the quay wall and the crane at t_{L1} is indicated in **Fig. 13**. The superstructure deforms mainly horizontally at this time. This vibration is the first mode of the crane so that legs deform most. Rotational deformation at Node B and C are greater than the other part of legs and the local buckling there occurred by the large bending moments.

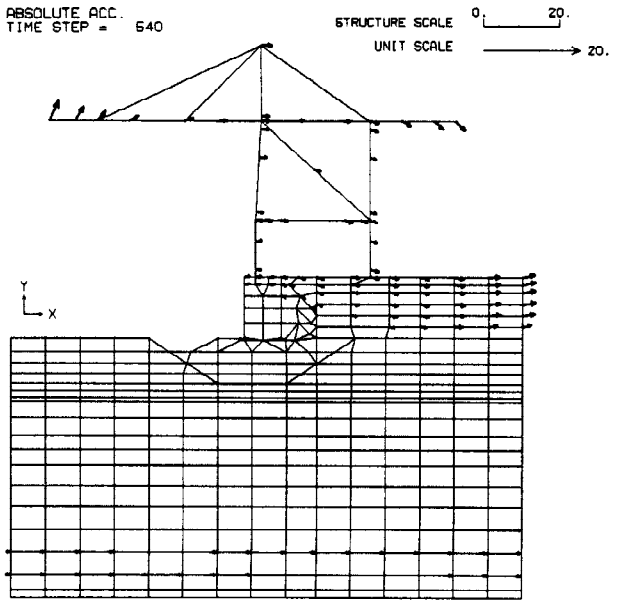

Fig. 12 Acceleration vectors of quay wall and crane at t_{L1} (unit:m/sec^2)

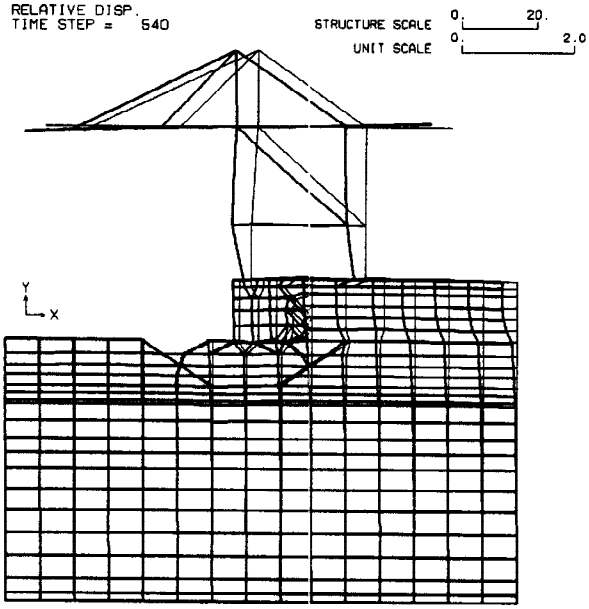

Fig. 13 Deformation of quay wall and crane at t_{L1} (unit:m)

EFFECT OF INTERACTION BETWEEN QUAY WALL AND CRANE

From the analyses for a quay wall model and for an interaction model of both a quay wall and a crane, **Fig. 14** express horizontal accelerations at a seaside rail (solid line) and a landside rail (broken line). The upper and lower figures are results of the interaction model and the quay wall model. These figures indicate only for the first 10 sec in total analytical time 30 sec.

In both results, the seaside and the landside rail vibrate at the approximately same phase. Comparing with the maximum acceleration at t=4.04 sec, the landside rail is a little larger than the seaside rail. Moreover, the acceleration at both rails are amplified than the acceleration at a surface of the free field KP+04 (referring to top of **Fig. 9**). This amplification is explained by the reason that the shear rigidity in the vicinity of the caisson and the reclaimed ground decrease less than the free filed, although both rails are set on the caisson and the reclaimed ground of larger rigidity. In comparison with acceleration waves at the seaside and the landside rail between the upper and the lower figures, the maximum acceleration and the time for the quay wall model agree with them for the interaction model.

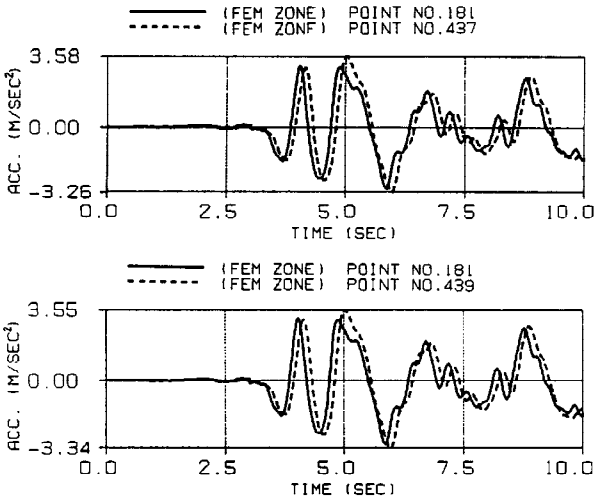

Fig. 14 Acceleration waves at both a seaside rail (solid line) and a landside rail (broken line) for a quay wall model and an interaction model

Fig. 15 shows a ratio of a transfer function for the quay wall model to a transfer function for the interaction model at the seaside rail (solid line) and the landside rail (broken line). Therefore, the ratio is 1.0 if transfer functions for both analytical models are the same in the frequency domain. The ratio at f=0.5 Hz, which corresponds to the natural frequency of the crane, decrease in this figure. This indicates that the interaction affects the acceleration response, because the crane confines the vibration of the quay wall. However, the ratio may approach 1.0 after the rocking starts as a leg is lifted up.

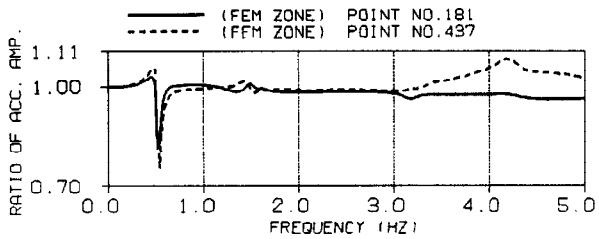

Fig. 15 Ratio of a transfer function for a quay wall model to a transfer function for an interaction model

CONCLUSIONS

1)Main causes of damage for cranes are considered to be lateral deformation of caissons and rocking vibration of cranes.

2)This analysis method is not enough to estimate deformation of quay walls, because the program can not consider the slip of the structure and the failure and the liquefaction in the ground. However, the acceleration can be easily estimated by this method.

3)Local buckling can be considered to occur around nodes in legs due to the rocking vibration.

4)The dynamic behaviors of the quay wall and the crane are clarified. In the design standard, the interaction depending on the ground and the structure should be considered.

REFERENCES

Coastal Development Inst. of Tech. (1993). *Handbook on Liquefaction Remediation of Reclaimed Land* (Port and Harbor Research Inst., ed), pp.50-59. (in Japanese)

Lysmer, J., T. Udaka, C. Tsai and H. B. Seed (1975). FLUSH, A Computer Program for Approximate 3-D Analysis of Soil-Structure Interaction Problems, *EERC* **75-30**.

Sugito, Sekiguchi, Yashima, Oka and Taguchi. Correction of vertical array strong motion data for buried directions and amplification characteristics of the ground. (to be published)